RSC Advances

PAPER

View Article Online
View Journal | View Issue

Cite this: *RSC Adv.*, 2025, **15**, 8707

A dual turn-on–off fluorometric probe based on silver sulfide quantum dots for simultaneous assay of creatinine and calcium in complex matrices

Hagar A. Moustafa,[a] Ahmed S. Abo Dena*[ab] and Ibrahim M. El-Sherbiny *[a]

Biomarkers like creatinine (**CRE**) and calcium ions (Ca^{2+}) are vital for detecting several disorders like chronic kidney disease (CKD). Hypocalcemia affects bones, the heart, and other organs. The main limitations of traditional **CRE**/Ca^{2+} monitoring protocols in biological samples are their invasiveness and time consumption. The present work aims at developing a rapid, highly sensitive, and selective fluorescent probe for the simultaneous determination of **CRE** and Ca^{2+} in pure and complex samples. The probe is based on Ag_2S quantum dots (QDs) modified with polyethyleneimine and imidazole dicarboxylic acid. The interaction of the analytes with the modified Ag_2S QDs causes a quenching in their fluorescence intensity at λ_{em} of 485 nm (λ_{ex}: 240 nm) and 605 nm (λ_{ex}: 300 nm) for **CRE** and Ca^{2+}, respectively. The system was characterized with high-resolution transmission electron microscopy, FTIR spectroscopy, dynamic light scattering, and zeta potential measurement. The influence of solution pH, incubation time, amount of modified QDs, and interfering species was investigated. The probe demonstrated a limit of detection of 0.48 and 0.45 μg mL^{-1}, a linear range of 0.7–9.0 and 0.5–4.0 μg mL^{-1}, and recovery values in the ranges of 93.8–98.4 and 94.2–103.6% for **CRE** and Ca^{2+}, respectively. The developed system can help in the early diagnosis of several renal disorders.

Received 7th January 2025
Accepted 7th March 2025

DOI: 10.1039/d5ra00164a

rsc.li/rsc-advances

Introduction

Kidneys are vital organs for blood filtration and urine excretion for toxins and waste clearance. Creatinine (**CRE**, Scheme 1) is a metabolic waste of proteins and muscles. Based on gender, age, and total muscle mass, the normal **CRE** level in adults is 5–11 μg mL^{-1} in women and 6–12 μg mL^{-1} in men.[1] Individuals who suffer from diabetes, obesity, hypertension, stress, an unhealthy lifestyle, alcoholism, age, and a family history of chronic kidney disease (CKD) are more likely to have kidney disease symptoms such as nausea, decreased mental activity, decreased urine production, and flank discomfort.[2] Many studies have linked CKD, the life-threatening disorder, with the low level of plasma calcium ions (Ca^{2+}),[3] as the kidney converts vitamin D (Vit D) into its active form which is responsible for absorbing Ca^{2+} from digested food. Impaired kidneys do not support this function well, resulting in low levels of Ca^{2+} in the circulating blood because of low levels of activated Vit D. Calcium is a mineral that is normally stored in bones. Only about 1% of Ca^{2+} exists in the circulation in one of two forms, namely, free Ca^{2+} (not linked to any plasma components) and bound Ca^{2+} (linked to albumin or other proteins in the plasma). This mineral is required for bone and teeth formation, helps in muscle contraction and blood clotting, as well as keeps heartbeats stable, and aids nerves to function properly. Accordingly, decreased levels of Ca^{2+} harm bones and affect heart and nerve functions.

Quantitative data for **CRE** levels can be obtained from Jaffe's method in an alkaline medium,[4] where **CRE** produces an orange product upon reaction with picric acid. The Ca^{2+} levels can be obtained from common laboratory tests for total and ionized Ca^{2+}.[5] Standard blood and urine tests are accepted worldwide, even though they are invasive, time-consuming, expensive, and not available all the time in hospitals. So, nanosensors, including fluorescent probes, have been widely applied in the last decades to overcome these limitations. The recent progress in nanoscience has led to the development of many techniques, including those depending on molecularly imprinted polymers (MIPs),[6] electrochemiluminescence (ECL),[7] surface plasmon resonance (SPR),[8] and quantum dots (QDs)-based methods[9] for sensing various biomarkers such as Ca^{2+} and **CRE** with high accuracy, sensitivity, and selectivity. Nanomaterial-based sensors are widely applied for the early diagnosis of many diseases because they can sense analytes in extremely low concentrations in plasma, urine, sweat, and saliva samples in a non-invasive way.

Quantum dots (QDs) are semiconductors of controllable nanoscale size with characteristic inherent fluorescence properties, so they have been widely utilized as label-free fluorescent probes. Their fluorescence intensity is enhanced or quenched based on the analyte's nature and concentration. In addition, QDs

[a]*Nanomedicine Laboratories, Centre for Materials Science, Zewail City of Science and Technology, 6th of October City, Giza, Egypt. E-mail: ielsherbiny@zewailcity.edu.eg*
[b]*Pharmaceutical Chemistry Department, National Organization for Drug Control and Research (NODCAR), Giza, Egypt*

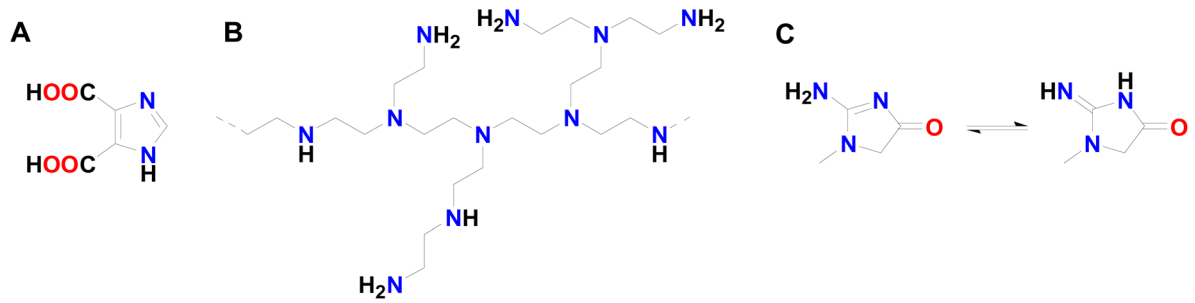

Scheme 1 The chemical structure of (A) 4,5-imidazole dicarboxylic acid (**IDCA**), (B) polyethyleneimine (**PEI**), and (C) creatinine.

can transfer the fluorescence excitation energy to another particle (*i.e.*, acceptor particle) in a process known as fluorescence resonance energy transfer (FRET). If the acceptor is non-fluorescent, this causes a total or partial turning off (quenching) effect on the fluorescence signal of QDs. In contrast, if the acceptor is fluorescent, FRET occurs, which causes the fluorescence of the QDs to decrease while that of the acceptor to increase. Therefore, this process occurs between QDs, acceptor particles, and the analyte, which either binds the QDs with the acceptor particles or separates them, causing a turn-on–off effect.[10]

A QDs-based paper strip dual-nanosensor was developed and reported for the detection of **CRE** and copper (Cu) ions *via* a mobile application.[11] The method demonstrated high sensitivity and selectivity potential for **CRE**/Cu detection in pure solutions and plasma samples. However, it is based on cadmium, which is a hazardous substance that may lead to serious environmental and human health concerns.

The present study is the first to use the safe and eco-friendly Ag_2S QDs coated with polyethyleneimine (**PEI**), a hyperbranched polymer with terminal primary amino groups, and 4,5-imidazole dicarboxylic acid (**IDCA**) (Scheme 1a and b) as a sensing element for dual determination of **CRE**/Ca^{2+} in pure and plasma-mimicking samples at different excitation wavelengths. The study also aims at investigating how different analyte concentrations at different pH values will affect the fluorescence signal of QDs in the presence of a complex matrix to study the probes sensitivity and selectivity towards **CRE** and Ca^{2+}. It is presumed that the fluorescence intensity of QDs will be quenched by increasing **CRE**/Ca^{2+} concentration in a linear manner. Therefore, one of the main aims of the present study is to propose a fluorescent probe that allows for rapid diagnosis and monitoring of first-degree CKD and other **CRE**/Ca^{2+} related diseases depending on the measurement of the changes in the fluorescence bands.

Experimental

Reagents and materials

All chemicals utilized in the present study are of analytical grade and were used without any purification. **CRE** pure solution (20 μg mL^{-1}) (Biomed Diagnostics, Hannover, Germany) was used to prepare the working solutions throughout the study. Silver nitrate ($AgNO_3$), sodium sulfide (Na_2S), sodium hydroxide (NaOH), hydrochloric acid (HCl), copper chloride ($CuCl_2$), urea, dextrose, iron(III) chloride hexahydrate ($FeCl_3 \cdot 6H_2O$), sodium bicarbonate ($NaHCO_3$), and sodium citrate were obtained from Fisher Scientific, Germany. Branched polyethyleneimine (**PEI**, approximate M.W. of 60 000) and 4,5-imidazole dicarboxylic acid (**IDCA**) were obtained from Acros Organics. Sodium chloride (NaCl) (PioChem), anhydrous monobasic sodium phosphate (NaH_2PO_4, Oxford Lab Chem), and anhydrous dibasic sodium phosphate (Na_2HPO_4, Loba Chemie) were used for preparing buffer solutions. Calcium chloride ($CaCl_2$) and potassium chloride (KCl) were purchased from Sigma-Aldrich, Germany. Double distilled water was used for aqueous solution preparation throughout the work.

Instruments

Transmission electron micrographs of the prepared fluorescent probe were obtained by utilizing a JEOL JEM-1010 transmission electron microscope operating at 80 kV (Regional Centre for Mycology and Biotechnology (RCMB), Al-Azhar University, Cairo, Egypt). On the carbon-coated copper grids (CCG), a drop of the sample suspension was applied, and it was dried by allowing the water to evaporate at room temperature.[12] A Nicolet iS10 Fourier-transform infrared spectrometer was operated in the transmission mode over the spectral window of 600–4000 cm^{-1} to study the chemical modification of the fluorescent Ag_2S QDs with **PEI** and **IDCA**. In addition, zeta potential (ZP) measurement and dynamic light scattering (DLS) techniques (Malvern Instrument) were used to measure the QDs' total charge and particle size before and after functionalization with **PEI** and **IDCA**. Moreover, fluorescence emission peaks were recorded using an RF-6000 spectrofluorophotometer (Shimadzu, Japan).

Preparation of CRE and Ca^{2+} solutions

Working solutions of **CRE** and Ca^{2+} were prepared from pure standard solutions of 20 and 2000 μg mL^{-1}, respectively. The working solutions were prepared by adding certain volumes of **CRE** (50–300 μL) or Ca^{2+} (400–900 μL) standard solutions and completing the final volumes to 2 mL with double distilled water. The mixtures were shaken well to make them homogeneous, and the resulting solutions were treated with the required additives (buffer solution and QDs) in order to investigate the sensor performance.

Phosphate buffer saline solution preparation

Phosphate buffer saline was prepared by dissolving accurately weighed 1.454 g of anhydrous Na_2HPO_4 and 0.353 g of

anhydrous NaH_2PO_4 in 100 mL of double distilled water. Thereafter, the solution mixture was divided into ten equal portions, and the pH was adjusted to 2, 3, 4, 5, 6, 7, 8, 9, 10, and 12.5 using dilute HCl or NH_4OH solutions.

Plasma-mimicking matrix

To investigate the selectivity of the proposed fluorescent probe towards **CRE** and Ca^{2+}, and to study the effect of matrix-interfering species on its performance, a plasma-mimicking solution was prepared. Briefly, 450 mg of NaCl, 21 mg of KCl, 25 mg of $NaHCO_3$, 25 mg of dextrose, 20.27 μL of $FeCl_3 \cdot 6H_2O$ solution (4.15 mg mL^{-1}), and 11.4 μL of urea solution (2.65 mg mL^{-1}) were added to 50 mL of double distilled water and shaken well to obtain a transparent true solution. To the above solution, an amount of $CaCl_2$ (12 mg) was added in the case of investigating the selectivity towards **CRE** and 12 μL of **CRE** solution (20 μg mL^{-1}) were added in the case of investigating the selectivity of the proposed fluorescent probe towards Ca^{2+} ions. Appropriate volumes of the above solutions were added during the assay of Ca^{2+} and **CRE** in pure and plasma-mimicking solutions.

Preparation of the modified Ag_2S QDs

With slight modifications to the Ag_2S QDs synthesis procedure reported elsewhere,[13] **IDCA**/**PEI**-functionalized Ag_2S QDs (modified Ag_2S QDs) were prepared. In separate tubes, 0.1 g of $AgNO_3$, 0.1 g of sodium citrate, and 0.2 g of Na_2S were dissolved in 50 mL, 50 mL, and 100 mL of double distilled water, respectively. The process was carried out in the dark and at ambient temperature. Accurately measured 50 mL of silver nitrate and 50 mL sodium citrate solutions were mixed first with 0.22 g of highly branched **PEI**, followed by the addition of 100 mL of sodium sulfide solution. The color of the mixture changed immediately from faint yellow to dark brown. The mixture was stored in the dark for 3 days to ensure the complete production of the modified Ag_2S QDs. The resulting suspension was centrifuged for 15 min at 9500 rpm and washed thrice with 10 mL of double distilled water. Thereafter, the supernatant was discarded and replaced with the smallest volume of double distilled water to be ready for lyophilization.[14] The **IDCA** solution was prepared by dissolving 10 mg of **IDCA** in 50 mL of double distilled water, and then 10 mL of this solution was added to 20 mg of the lyophilized modified Ag_2S QDs and stirred for 2 hours, washed well with double distilled water, and lyophilized. Accurately weighed 10.6 mg of the lyophilized modified Ag_2S QDs was dispersed in 100 mL of double distilled water to prepare a 106 μg mL^{-1} probe nanosuspension. Later, the obtained nanosuspension was used in the assay of **CRE** and Ca^{2+} in pure and plasma-mimicking samples. Fig. 1 demonstrates the synthesis procedures of the modified Ag_2S QDs.

Validation of the fluorescent probe

Validation is a strategy applied to confirm that an analytical procedure is appropriate to serve as a tool for quality assurance. Any analytical technique aims to produce accurate, reliable, and consistent analytical results. Precision, accuracy, linearity, linear range, limit of quantification (LOQ), and limit of detection (LOD) assessments are all part of the validation process of a specific analytical technique. An essential component of any effective analytical practice is the capacity to moderate the quality, consistency, and dependability of the analytical results using the findings from method validation.[15]

In the present study, various tests were necessary to investigate the system sensitivity and selectivity, like how the QDs amount and incubation time will affect the sensing process, the effect of pH changes on the interaction between the modified Ag_2S QDs and **CRE** and/or Ca^{2+}, and how QDs can sense these analytes within a complex matrix.

Because QDs have a larger molar absorption coefficient and quantum yield than typical organic fluorophores, they appear 20 times brighter and are hundreds of times more robust against photobleaching.[16] Increasing the concentration of QDs has the main role in improving the fluorescence intensity. Several solutions containing 50, 100, and 150 μL of the modified QDs suspension were used to study the effect of increasing the amount of modified QDs.

As the duration of the QDs synthesis process affects their size and main characteristics,[17] the incubation time of the modified QDs with the analytes of interest may also have a significant influence on the fluorescent signal. In order to investigate the effect of incubation time of the modified QDs with **CRE** and/or Ca^{2+} solutions on the performance of the proposed fluorescent probe, a mixture of 1.5 mL of double distilled water, 50 μL of the modified Ag_2S QDs suspension, and 50 μL of **CRE** working solution was scanned over the specified spectral window after different incubation periods (1–40 min).

Most chemical and biochemical reactions are highly affected by changes in solution pH. Besides, the morphology, structure, and stability of nanomaterials are only a few aspects of the great impact of the medium pH.[18] To study the performance characteristics of the proposed fluorescent probe with the variations in the solution pH, a set of 10 Eppendorf tubes was filled with 1.5 mL of the previously prepared phosphate buffer solutions of pH 2–12.5, 50 μL of the analyte, and 50 μL of the modified QDs suspension, and another Eppendorf tube containing 1.5 mL of pure distilled water was used as a blank.

Tang and Kebarle defined matrix effect as the distinction between an analyte's spectrometric reaction in standard solutions and its response in biological samples, such as serum, plasma, or urine, which can be impacted by factors including the target analyte, sample preparation technique, composition, and choice of the equipment.[19–21] It can be especially noticeable in complicated mixtures when the target molecules interfere with other species, thus changing the quantitative outcomes of the assay. This might influence the consistency, linearity, effectiveness, preciseness, and sensitivity of the analytical technique.[22] Monitoring the modified QDs' behavior in the presence of Ca^{2+} and **CRE** analogues is an important assessment. Accordingly, 50 μL of each interfering species (Cu^{2+}, Fe^{3+}, glucose, K^+, Na^+, Zn^{2+}, and urea) were added to 50 μL of the analyte solution (**CRE** or Ca^{2+}), and 50 μL of the modified QDs suspension in 1.5 mL of distilled water to examine the effect of these interfering species on the probe's selectivity toward **CRE** and Ca^{2+}.

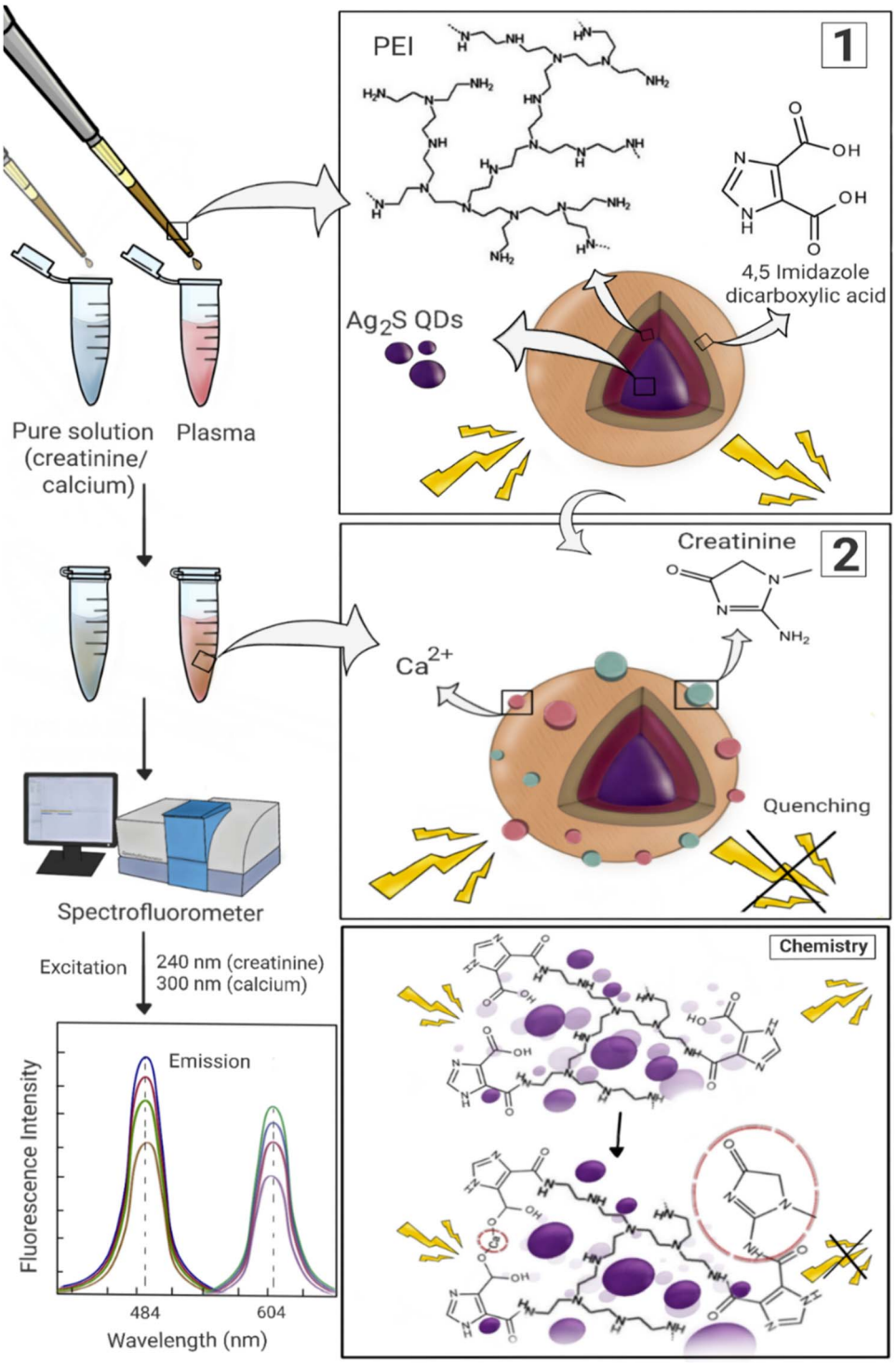

Fig. 1 The composition of the modified Ag_2S QDs and their response to the presence of **CRE** and Ca^{2+}.

Several strategies may be applied to decrease or completely eradicate matrix effect by altering ionization, enhancing extraction and cleanup methods, and using corrective calibration techniques.[21] Besides, the standard addition method is usually applied in analytical chemistry to overcome the influence of the complex matrix that exists in blood and biological samples.[15,23,24] So, a solution very similar to Ringer's solution was prepared to mimic the real components of plasma. In the case of **CRE**, 3 mL of the plasma-mimicking solution, 1 mL of BPS buffer of pH 4, 200 μL of the modified QDs suspension, and 50 μL of the unknown **CRE** or Ca^{2+} solutions were mixed well. Following, 50 μL of **CRE** standard solution (0.5–6 μg mL^{-1}) or 50 μL of Ca^{2+} standard solution (10–100 μg mL^{-1}) were added, and the fluorescence signal was measured at λ_{em} of 485 nm (λ_{ex}: 240 nm) and 605 nm (λ_{ex}: 300 nm) for **CRE** and Ca^{2+}, respectively. Eventually, in the case of pure sample solutions, all the above

procedures were applied except for the addition of the plasma-mimicking solution. Alternatively, the solution volume was completed with the same volume of PBS buffer of pH 4.

Results and discussion

Electron micrographs

Transmission electron microscopy was used to investigate the size, morphology, and surface coating of the Ag_2S QDs. Both unmodified (plain) and modified/functionalized Ag_2S QDs were imaged, and the surface coating with **PEI** was proved. The plain Ag_2S QDs (Fig. 2A and B) and the **PEI**-coated Ag_2S QDs (Fig. 2C and D) demonstrate a well-defined spherical shape with comparable sizes. On the other hand, the **PEI**-modified Ag_2S QDs exhibited a polymeric layer around individual or aggregated particles appearing as a flare (magnified inset in Fig. 2C) due to the lower density of the polymer compared to the inorganic metal sulfide QDs, thus confirming the successful modification with **PEI**. Moreover, both plain and modified Ag_2S QDs show a homogeneous particle size less than 35 nm.

FTIR analysis

FTIR is a spectroscopic chemical analysis technique used to characterize compounds through scanning across test samples to evaluate their chemical characteristics.[25,26] The **PEI** and **IDCA** (Scheme 2) are responsible for the chemical interaction of the modified Ag_2S QDs with **CRE** and Ca^{2+}. The FTIR spectra of plain, **PEI**-modified, and **IDCA/PEI**-modified Ag_2S QDs were recorded to confirm the successful synthesis of the proposed functionalized fluorescent probe (Fig. 3).

The FTIR spectrum of the plain Ag_2S QDs revealed characteristic bands at 669 and 1106 cm^{-1} indicating the presence of sulfide. In addition, the absorption bands at 1558–1456 cm^{-1} correspond to the C=O stretching of the carboxylic groups.[27] The **PEI**-modified Ag_2S QDs demonstrated a characteristic broad band at 3200–3500 cm^{-1} corresponding to O–H stretching vibration. Other characteristic bands at 2900 and 2798 cm^{-1} are attributed to alkane C–H stretching. Moreover, C=O stretching, N–H bending, secondary amine N–H bending, and the aliphatic nitro groups are indicated by the appearance of absorption bands at 1735, 1654, 1560, and 1541 cm^{-1}, respectively.[28,29] However, in the case of **IDCA/PEI**-modified Ag_2S QDs, the sharp band at 3171 cm^{-1} indicates an aromatic C–H stretching. Furthermore, aromatic C–H bending, C=N bending, amide II, and amide III bands were recognized at 1887, 1455, 1576, and 1250 cm^{-1}, respectively.[30,31] The presence of amide II and III bands indicates the successful binding of **IDCA** to **PEI** *via* amide bond formation. Based on these spectroscopic results, the main functional groups present in the studied structures are –COOH and $–NH_2$ in **IDCA** and **PEI**, respectively. So, it is hypothesized that **PEI**-modified Ag_2S QDs have free primary amine groups that condense with one of the free carboxyl groups of **IDCA** with the removal of a water molecule to give the final **IDCA/PEI**-modified fluorescent Ag_2S QDs. Additionally, the principle of **CRE** and Ca^{2+} sensing also

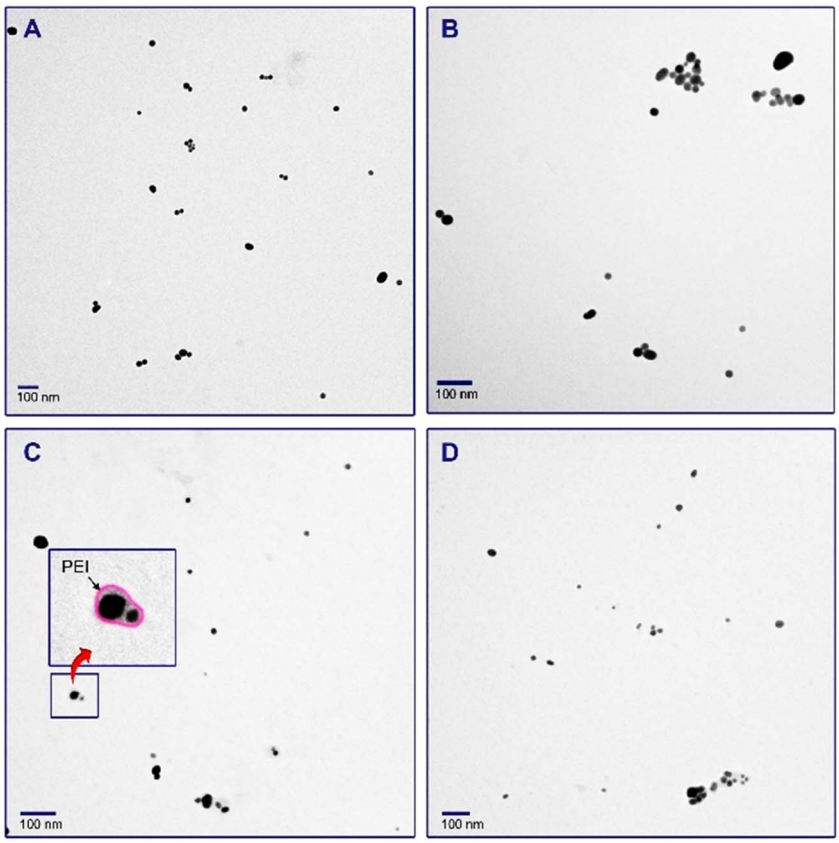

Fig. 2 TEM micrographs of plain (A and B) and surface modified (C and D) Ag_2S QDs.

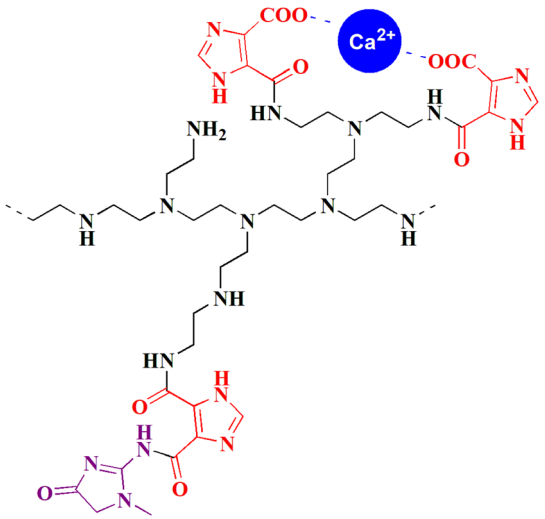

Scheme 2 A schematic illustration of the binding of the amine groups of PEI (black) to the carboxylic groups of IDCA (red), and binding of the amino groups of CRE (purple) to the carboxylic groups of IDCA. The Ca^{2+} ions (blue) are interacting with two free carboxylate groups of two IDCA molecules.

depends on the free functional groups. **CRE** has a free amino group that covalently binds to the second carboxyl group of **IDCA**. On the other hand, Ca^{2+} ions have a high affinity to carboxylate groups due to their two positive charges.[32] However, there is no doubt that nonspecific physical interactions may also occur between the analytes and the modified Ag_2S QDs. Both chemical and physical interactions quench the fluorescence intensity of the fluorescent probe in response to increasing the concentration of the analytes. Scheme 2 depicts the possible interactions of **CRE** and Ca^{2+} with the functional groups on the modified Ag_2S QDs.

Particle size and zeta potential

Information about particle size and surface charge was obtained using dynamic light scattering (DLS), and through measuring the zeta potential, respectively (Fig. 4). The average particle size of plain Ag_2S QDs was found to be 86 nm. In addition, the **PEI**-functionalized Ag_2S QDs exhibited an average particle size of 98 nm. A larger particle size was obtained in the case of **IDCA**/**PEI**-modified Ag_2S QDs which demonstrated an average size of 131 nm. The increase in the average particle size confirms the successful modification with **PEI** followed by **IDCA**. It is worth mentioning that the difference between the particle size obtained from TEM imaging and that obtained from DLS measurement is attributed to the fact that DLS measures the average particle size in suspension, while TEM measures individual dried particles. Besides, the size obtained from DLS is affected by many factors such as sample concentration, the type of solvent, and the stability of the nanoparticle suspension. Moreover, aggregation of the nanoparticles may occur, resulting in a false increase in the average particle size.

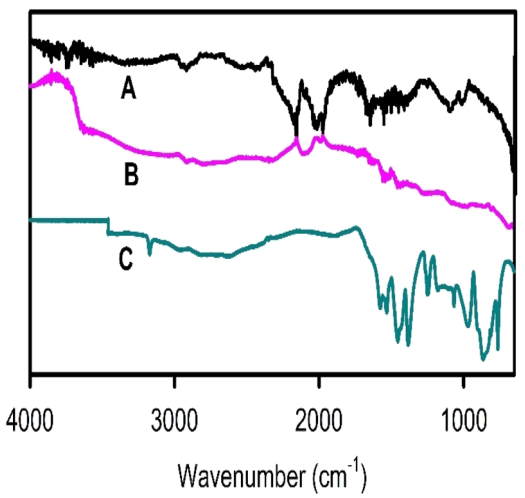

Fig. 3 FTIR spectra of (A) unmodified (plain) Ag_2S QDs, (B) **PEI**-coated Ag_2S QDs, and (C) **IDCA**/**PEI**-modified Ag_2S QDs.

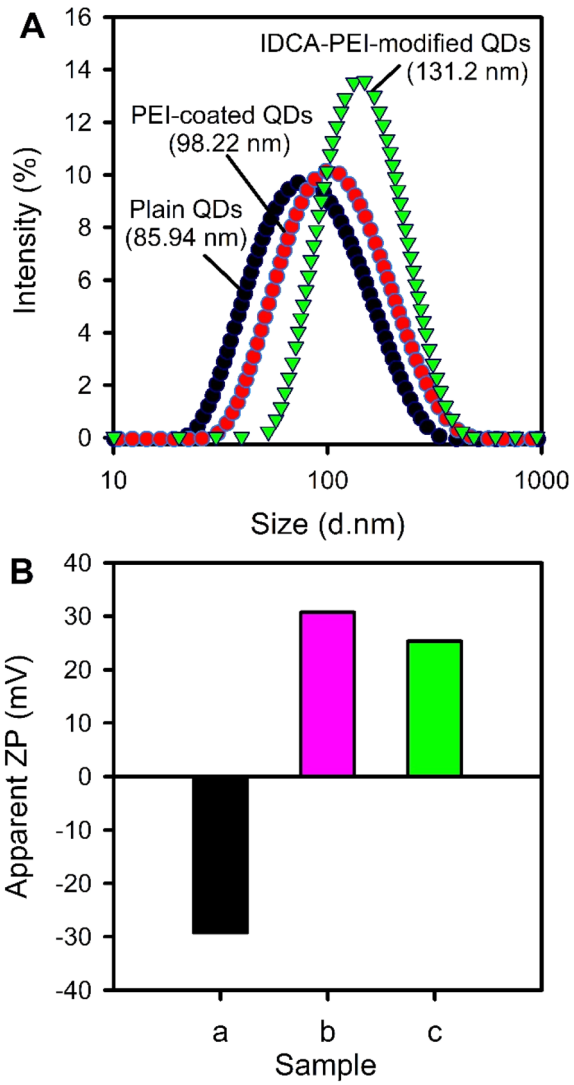

Fig. 4 (A) DLS results for measuring the particle size of plain, **PEI**-modified, and **IDCA**–**PEI**-modified QDs; (B) zeta potential values of plain (sample a), **PEI**-modified (sample b), and **IDCA**/PEI modified (sample c) Ag_2S QDs.

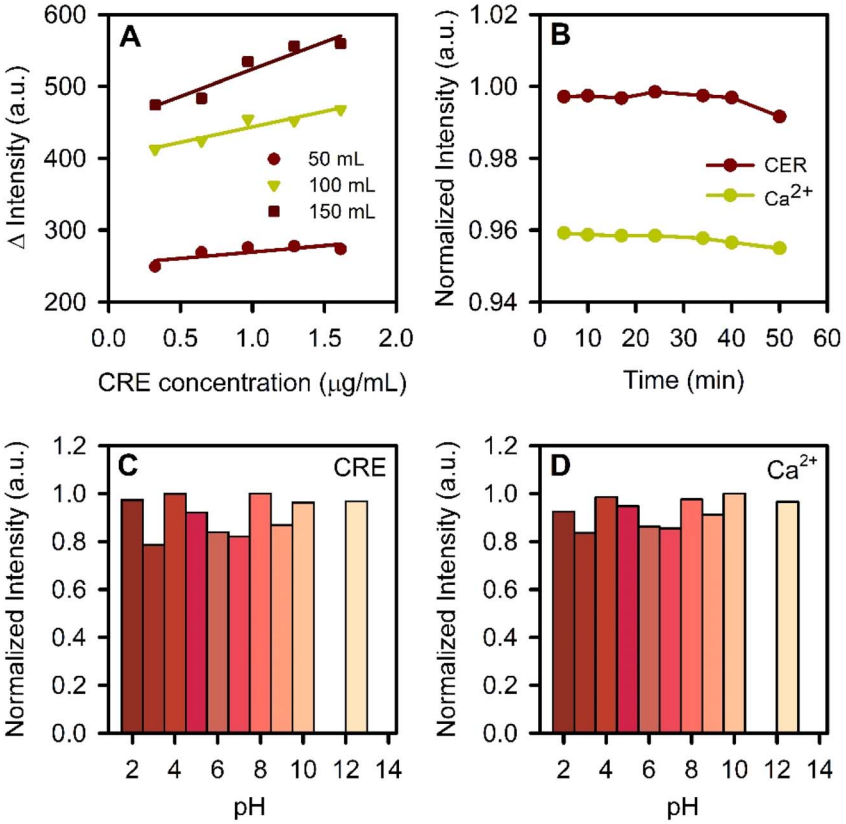

Fig. 5 (A) Effect of QDs amount, and (B) effect of incubation time (over 50 min incubation period) on the fluorescence intensity of the modified QDs. (C) and (D) effect of pH on the fluorescence intensity of the proposed fluorescence probe in the case of **CRE** and Ca^{2+}, respectively.

Therefore, it is recommended to measure the individual particle size with the aid of TEM imaging.

To further confirm the functionalization of plain Ag_2S QDs, changes in zeta potential were measured before and after functionalization. The positive charges of **PEI** and the negative charges of **IDCA** are supposed to have a clear influence on the zeta potential of the plain Ag_2S QDs. The zeta potential of plain Ag_2S QDs was found to be −29.2 mV, and that of **PEI**-functionalized Ag_2S QDs was found to be +30.7 mV. This very large shift in zeta potential towards a large positive value confirms the successful modification of the Ag_2S QDs with **PEI**. Moreover, the **IDCA**/**PEI**-modified Ag_2S QDs showed a zeta potential of +25.35 mV, with a less positive value compared to that modified with **PEI** alone, which reflects the role of the negatively charged **IDCA**. This confirms that the modification of **PEI**-functionalized Ag_2S QDs with **IDCA** was successfully achieved.

Influence of QDs amount

Ag_2S QDs are among the best nanomaterials for developing fluorescent nanosensors since they do not include heavy metals like lead, cadmium, or mercury, and they satisfy safety, health, and environmental requirements. The primary field in which Ag_2S QDs have been used is biological imaging.[33] The amount of QDs nanosuspension added to the analyte's test solution is one of the factors that must be investigated during optimizing the sensing conditions. Intuitively, it was found that increasing the volume of the added nanosuspension of the modified Ag_2S QDs provides higher fluorescence intensity for the best detection of **CRE**/Ca^{2+} (Fig. 5A). It is clear from the results in Fig. 5A that the best amount of the modified Ag_2S QDs suspension that gives the highest fluorescence intensity is 150 μL.

Incubation period

The required time for the synthesis process has a significant impact on the type and characteristics of nanoparticles that are manufactured. The properties of the generated nanoparticles may change over time and be significantly impacted by the methods used during production, contact with light, storage settings, and other factors. There are several ways that temporal differences might happen in response to time, including particle accumulation from prolonged preservation, particle growth or shrinkage, shelf life, and other factors that influence the potential of the particles.[17,34,35] The synthesis procedure of the modified Ag_2S QDs required incubation for three days to ensure the maximum QDs production, and then the **IDCA** modification step was done on day 4, and the resulting QDs were reconstituted in double distilled water for subsequent use. The suspension showed good stability during the course of the study.

Regarding the incubation time, the fluorescence intensity was recorded over a period of 50 min to determine the optimum time that allows the reaction between **CRE**/Ca^{2+} and the probe QDs. The fluorescence intensity showed an insignificant change over

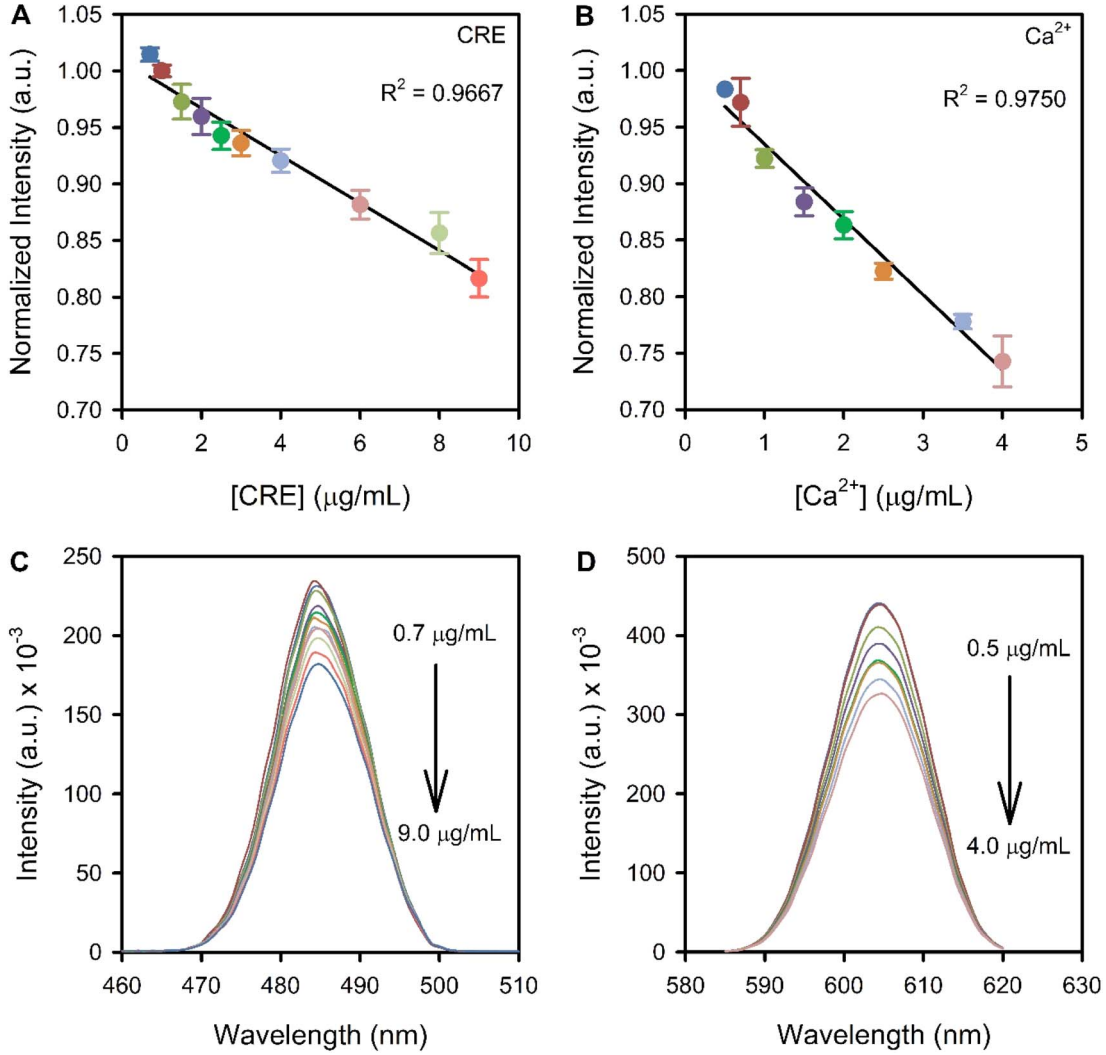

Fig. 6 Standard curves and their corresponding emission spectra for the determination of **CRE** (A and C) and Ca^{2+} (B and D) in pure solutions. The arrows indicate the direction of increasing **CRE** or Ca^{2+} concentration.

time (Fig. 5B). Therefore, all the subsequent measurements were performed after 5 min of incubation of the modified Ag_2S QDs in the analyte sample solution. This allows for rapid analysis of **CRE** and Ca^{2+} compared to many other analytical methods that may require longer sample preparation and incubation periods.

Sample solution pH

It is necessary to investigate the significant impact of pH on the reaction between the fluorescent modified QDs and the analytes of interest. The production and properties of nanoparticles, particularly metal, metal oxide, and metal sulfide nanoparticles, are significantly influenced by the medium pH. The pH and temperature are important factors affecting the solubility of metals since they have a great influence on the quantity of the reducing functional groups in the reducing agent that may alter the output of nanoparticle formation. High reduction rates are observed at high pH during nanoparticle production. The reduction processes will be exceptionally rapid at a basic pH (over 9 or 10), which will cause the nanoparticles to aggregate.[18,36] The modified Ag_2S QDs were prepared in aqueous media at a pH of 8.

On the other hand, the pH of the reaction medium may significantly influence the interaction of **CRE** and Ca^{2+} with the modified QDs. Fig. 5C and D depict the influence of pH on the fluorescence intensity of the modified QDs in the presence of **CRE** or Ca^{2+}, respectively. It was found that the intensity of the fluorescence signal does not demonstrate a significant change when the pH of the solution was changed over the range of 2–12.5. These findings indicate that both **CRE** and Ca^{2+} can be determined in a wide range of pH.

Analytical parameters

The probe's accuracy, precision, specificity, LOD, LOQ, linearity, and linear range are the main parameters that control its validity to be applied for **CRE**/Ca^{2+} detection and determination. Accuracy is the degree to which test findings closely resemble the real values, and it can be investigated by conducting the recovery test. The percentage recovery is determined by assaying

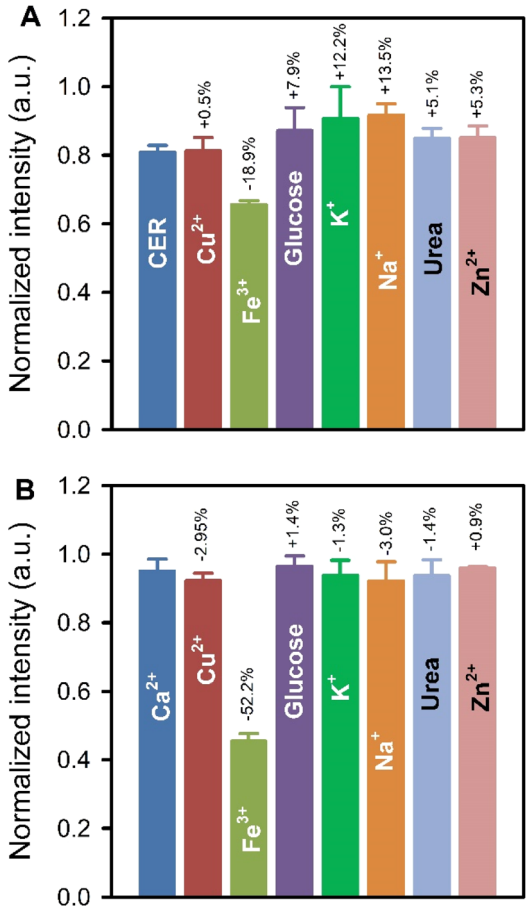

Fig. 7 The interference effect of different species on the interaction between the proposed fluorescent probes with CRE (A) and Ca^{2+} (B). The values above each column represent the percentage change in fluorescence intensity of the proposed probe, due to the presence of interfering species, with respect to the control CRE or Ca^{2+} signals.

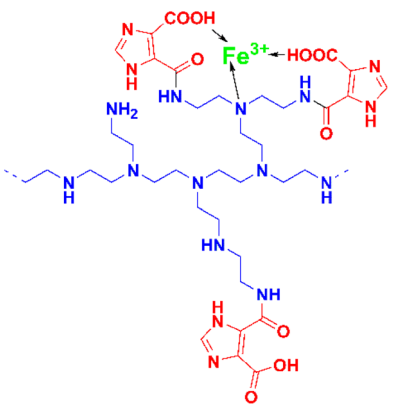

Scheme 3 Suggested mechanism of interaction between Fe^{3+} ions with PEI and IDCA on the surface of the modified Ag_2S QDs.

a known quantity of the analyte within the linear concentration range. In addition, a good indicator of the probe's precision is the degree of similarity between multiple measurements performed after repeatedly sampling the same standardized sample under the given circumstances. On the other hand, the probe's specificity is determined by its capacity to measure the analyte with accuracy and selectivity even when other substances that may be anticipated to be found in the sample medium are present. A technique that generates a result for only a single analyte is referred to as specific.

LOD is the lowest concentration of an analyte in a sample that can be identified but may not necessarily be quantified under specified experimental circumstances. However, the LOQ is the lowest quantity of the analyte in a sample that can be quantitatively determined and quantified with a respectable degree of accuracy and precision under the specified operating parameters of the technique. Moreover, the linearity of an analytical method is its capacity to produce test findings that are exactly proportionate to the concentration of the analyte in the sample, within a specified range. Furthermore, the range between the highest and lowest concentrations of the analyte with an appropriate degree of linearity and accuracy is referred to as the linear range of the analytical procedure.[15,37–39] The fluorescence properties of the modified Ag_2S QDs is highly affected by **CRE**/Ca^{2+}, and an obvious decrease in the fluorescence intensity can be observed by increasing the **CRE**/Ca^{2+} concentration (Fig. 6). This quenching indicates the chemical changes taking place on the surface of the modified Ag_2S QDs upon adding **CRE**/Ca^{2+} to the fluorescent probe's suspension.

Pure solutions of **CRE** in the concentration range of 0.7–9.0 μg mL^{-1}, and Ca^{2+} in the concentration range of 0.5–4.0 μg mL^{-1} were used to construct the standard curves (Fig. 6A and B). The plots of the standard curves showed linearity within the above ranges with R^2 values of 0.9667 and 0.9750 for **CRE** and Ca^{2+}, respectively. Moreover, the LOD was found to be 0.48 ± 2.11% (95% confidence interval = ±0.013) and 0.45 ± 3.43% (95% confidence interval = ±0.020) μg mL^{-1} for **CRE** and Ca^{2+}, respectively. However, LOQ values were found to be 6.20 and 1.60 μg mL^{-1} for **CRE** and Ca^{2+}, respectively. The values of standard deviation indicated the precision of the recommended analytical procedure.

Matrix interference

Biological samples like blood are composed of a complex matrix incorporating many cations and **CRE** analogs that may interfere with the sensitivity and selectivity of the proposed fluorescent probe. Seven interfering species were tested in order to investigate their influence on the sensitivity and selectivity of the proposed fluorescent probe towards **CRE** and Ca^{2+}. In the case of **CRE**, there was a slight insignificant change in the fluorescence intensity upon adding Cu^{2+}, Zn^{2+}, K^+, Na^+, glucose, and urea. Therefore, these species do not have a significant influence on the sensing ability or selectivity of the studied probe. However, Fe^{3+} demonstrated a higher effect on the measured fluorescence signal when added to the **CRE** sample, causing more quenching of the fluorescence (Fig. 7). Similar results were obtained in the case of Ca^{2+}, where all the investigated interfering species showed insignificant changes in the fluorescence signal resulting from the interaction of Ca^{2+} ions with the fluorescent probe, except for Fe^{3+} ions that showed the highest interference. So, it is highly recommended to apply the standard addition method to avoid matrix interference.

Table 1 Determination of **CRE** and Ca^{2+} in pure and plasma-mimicking solutions by direct calibration and standard additions methods

	Determination of **CRE**			Determination of Ca^{2+}		
Method of assay	Taken (ng)	Found (ng)	Recovery (%)	Taken (μg)	Found (μg)	Recovery (%)
Direct calibration (pure samples)	58	55.38	95.5 ± 0.29	0.50	0.50	100.7 ± 0.17
	103	96.66	93.8 ± 0.23	1.50	1.44	96.3 ± 0.20
	161	156.0	96.9 ± 0.19	3.00	2.83	94.2 ± 0.21
	200	196.7	98.4 ± 0.21	7.50	7.77	103.6 ± 0.19
	400	380.8	95.2 ± 0.24	10.5	9.90	94.3 ± 0.23
Standard addition (plasma-mimicking samples)	7.0	7.21	103.0 ± 0.3	0.5	0.49	98.0 ± 0.31
	190	180.6	95.1 ± 0.27	1.5	1.44	96.0 ± 0.35
	290	271.1	93.5 ± 0.24	3	3.03	101.0 ± 0.24
	1065	991.5	93.1 ± 0.28	7.5	7.56	100.8 ± 0.20
	1150	1143.6	99.4 ± 0.18	10.5	10.4	99.1 ± 0.25

Table 2 A summary of the analytical parameters of the proposed analytical method and selected **CRE** and Ca^{2+} analytical methods from the literature[a]

	Method	Linear range (mg L^{-1})	R^2	LOD (mg L^{-1})	Ref.
CRE	Fluorescence	0.11–13.57	0.995	0.008	41
	Microfluidics	50–10^3	>0.99	16.9	42
	Voltammetry	0.001–22.62	0.995	9×10^{-4}	43
	Voltammetry	0.11–226.24	0.997	3.4×10^{-3}	44
	Digital image colorimetry	0–0.566	0.996	5.66	45
	Colorimetry	3.39×10^{-5}-5.66×10^{-3}	0.976	2.2×10^{-5}	46
	UHPLC-MS/MS	0.11–7.24	0.995	1.9×10^{-3}	47
	Fluorescence probe	0.7–9.0	0.967	0.48	This work
Ca^{2+}	Plasma atomic emission spectroscopy	0–20	0.999	13.1	48
	Electrochemical sensor	0.03–0.13	0.994	6.4×10^{-5}	49
	Potentiometry	0.8–12	0.960	0.12	50
	Spectrophotometry	0–0.6	0.999	9.33×10^{-6}	51
	Optical sensor strip	0.8–3.1	0.989	0.20	52
	Derivative spectrophotometry	0.8–4.8	0.992	0.0575	53
	Paper-based analytical method	5 – 40	0.983	2.90	54
	Fluorescence probe	0.5–4.0	0.975	0.45	This work

[a] The values of concentration were converted to a unified unit to allow for easy comparison among the analytical methods.

The reduction of fluorescence signal due to interaction with Fe^{3+} ions was reported in the literature using a similar system. Zhao *et al.* studied the interaction of Fe^{3+} ions with **PEI** and polydopamine.[40] The study reported that the interaction results in complex formation, where the Fe^{3+} ions coordinate with the two polymers *via* the two oxygen atoms of the dopamine monomer and the nitrogen atom of **PEI**. This may provide information about the expected mechanism of interaction of Fe^{3+} ions with **PEI** and **IDCA** studied herein (Scheme 3). The binding of Fe^{3+} ions with the two oxygen atoms of **IDCA** and the nitrogen atom of **PEI** may be the reason behind the reduced fluorescence signal of the proposed fluorescent probe in the presence of ferric ions.

Assay of CRE and Ca^{2+} in plasma-mimicking samples

Exciton recombination is often linked to the fluorescence of QDs (electrons and holes). Its efficiency is influenced by changes in the outer state or receptor structure of QDs, which in turn affects the fluorescence efficiency. The indirect or direct interaction between QDs and the target has been the basis of research on QDs-based fluorescence sensors for decades. The linear correlation between the variations in QDs fluorescence intensity and the analyte concentration enables the quantitative measurement of target analytes. Thus, by altering the surface ligands of QDs, functionalized QDs could be obtained, and then QDs-based fluorescence sensors could be created by exploiting the fluorescence changes brought about by direct physical adsorption or chemical interaction between the target analyte and the small functional groups on the surface of the fluorescent QDs.[16]

CRE and Ca^{2+} concentrations can be estimated from the fluorescence intensity of the modified Ag_2S QDs utilized herein by applying the standard addition method, a widely used method in analytical chemistry, using **CRE** or Ca^{2+} standard solutions to determine the concentration of the unknown samples. In plasma-mimicking solutions, these trials revealed a sensitive detection ability with recovery values of 93.1–103.0 and 96.0–101.0% for **CRE** and Ca^{2+}, respectively. In addition, the analysed amounts of **CRE** and Ca^{2+} were very low (7–1150 ng of **CRE** and 0.5–10.5 μg of Ca^{2+}) as shown in Table 1. Moreover,

Table 2 depicts a summary of the analytical parameters of the present fluorescence probe and a number of methods selected from the literature.

Conclusions

Serum creatinine and calcium levels can play an important role in the early diagnosis of kidney function impairment. The present study provides a reliable analytical method for the simultaneous determination of **CRE** and Ca^{2+} in pure and plasma-mimicking samples. The proposed method relies on chemically modified silver sulfide quantum dots that have inherent fluorescence properties and showed a significant fluorescence quenching upon interacting with **CRE** and Ca^{2+}. The present fluorescent probe showed excellent sensitivity towards **CRE** and Ca^{2+} in pure samples. In addition, the probe proved excellent selectivity towards **CRE** and Ca^{2+} in plasma-mimicking samples; however, a minimal interference from Fe^{3+} ions was found, which may be attributed to the complex formation of Fe^{3+} ions with two oxygen atoms from **IDCA** and one nitrogen atom from **PEI**. Therefore, the standard addition method was applied in the case of low analyte concentrations and the presence of complex matrix components in order to eliminate the effect of the interfering species. Satisfying results were obtained in terms of low LOD, good linearity, and wide linear range relative to the previously reported analytical methods, except for some voltametric and potentiometric methods. However, the sensor has some advantages over these methods, including its ease of preparation, very low sample volume, multiplexed sensing, and very high sensitivity. One limitation of the sensor is its very high sensitivity, which magnifies the influence of random experimental errors. In addition, ferric ions may cause a relatively significant interference (*i.e.* quenching of the analytical signal) in complex biological samples, and this can be overcome by Fe^{3+} masking. This can be investigated in a subsequent study in order to study the mechanism of Fe^{3+} ion interaction with the probe, and how their effect can be eliminated. The proposed sensor can be utilized in the simultaneous determination of **CRE** and Ca^{2+} in biological samples with high accuracy, as revealed by the high recovery values obtained in the present study. There is a lack of research in the area of multiplexed sensing of biological analytes using fluorescent sensing probes. Therefore, future research should be devoted to the simultaneous determination of more than two analytes using a single fluorescent sensing probe.

Data availability

The authors confirm that the data supporting the findings of this study are available within the article and the raw data will be available on request.

Author contributions

HAM: methodology, investigation, writing–original draft. ASAD: conceptualization, methodology, investigation, formal analysis, data curation, visualization, writing–review and editing. IME: conceptualization, funding acquisition, resources, supervision, writing – review and editing, project administration.

Conflicts of interest

There are no conflicts to declare.

Acknowledgements

The corresponding author extends his appreciation to the Science, Technology and Innovation Funding Authority (STDF), Egypt, for funding and supporting this work through the funds (Capacity Building Fund, CB-22808 and STDF FLUG Call 1-Project ID 46715).

Notes and references

1 A. O. Hosten, in *Clinical Methods: the History, Physical, and Laboratory Examinations*, ed. Walker H. K., Hall W. D. and Hurst J. W., Butterworths, Boston, 3rd edn, 1990.
2 M. A. Brown, G. K. Collett, E. A. Josland, C. Foote, Q. Li and F. P. Brennan, *Clin. J. Am. Soc. Nephrol.*, 2015, **10**, 260–268.
3 Z.-H. Liu, G. Li, L. Zhang, J. Chen, X. Chen, J. Zhao and X. Liang, *Kidney Diseases*, 2019, **5**, 197–203.
4 J. R. Delanghe and M. M. Speeckaert, *NDT Plus*, 2011, **4**, 83–86.
5 L. Sava, S. Pillai, U. More and A. Sontakke, *Indian J. Clin. Biochem.*, 2005, **20**(2), 158–161.
6 S. M. Amininasab, P. Holakooei, Z. Shami and E. Jaliliyan, *J. Compos. Compd.*, 2022, **4**, 83–88.
7 U. Lad, S. Khokhar and G. M. Kale, *Anal. Chem.*, 2008, **80**(21), 7910–7917.
8 R. Janmanee, A. Baba, S. Phanichphant, S. Sriwichai, K. Shinbo, K. Kato and F. Kaneko, *ACS Appl. Mater. Interfaces*, 2012, **4**, 4270–4275.
9 S. Kumar and R. Singh, *Opt. Laser Technol.*, 2021, **134**, 106620.
10 M. K. Alenichev, A. A. Yushina, E. B. Drozhennikova, I. S. Filimonov, O. A. Baranova, A. V. Chekanov and A. D. Levin, *Meas. Tech.*, 2019, **62**, 784–789.
11 R. V. Nair, P. Radhakrishna Pillai Suma and R. S. Jayasree, *Mater. Sci. Eng., C*, 2020, **109**, 110569.
12 B. H. Amin, H. Y. Ahmed, E. M. El Gazzar and M. M. M. Badawy, *Dose-Response*, 2021, **19**(4), 15593258211059323.
13 S. I. Sadovnikov, *Russ. J. Inorg. Chem.*, 2019, **64**, 1309–1316.
14 S. I. Sadovnikov, *Russ. J. Inorg. Chem.*, 2019, **64**, 1309–1316.
15 S. Dagadu Chavan and D. M. Desai, *World J. Adv. Res. Rev.*, 2022, **16**, 389–402.
16 Z. Wang, B. Yao, Y. Xiao, X. Tian and Y. Wang, *Chemosensors*, 2023, **11**(7), 405.
17 J. K. Patra and K. H. Baek, *J. Nanomater.*, 2014, **2014**, 417305.
18 L. Enayati Ahangar, K. Movassaghi and F. Yaghoobi, *Iran. J. Chem. Chem. Eng.*, 2022, **41**, 2175–2188.
19 F. Raposo and D. Barceló, *TrAC, Trends Anal. Chem.*, 2021, **134**, 116068.

20 P. Panuwet, R. E. Hunter Jr, P. E. D'Souza, X. Chen, S. A. Radford, J. R. Cohen, M. E. Marder, K. Kartavenka, P. B. Ryan and D. B. Barr, *Crit. Rev. Anal. Chem.*, 2016, **46**, 93–105.
21 M. L. Williams, A. A. Olomukoro, R. V. Emmons, N. H. Godage and E. Gionfriddo, *J. Sep. Sci.*, 2023, **46**, 2300571.
22 M. Cortese, M. R. Gigliobianco, F. Magnoni, R. Censi and P. Di Martino, *Molecules*, 2020, **25**(13), 3047.
23 I. G. Zenkevich and I. O. Klimova, *J. Anal. Chem.*, 2006, **61**, 967–972.
24 J. E. T. Andersen, *TrAC, Trends Anal. Chem.*, 2017, **89**, 21–33.
25 S. A. Khan, S. B. Khan, L. U. Khan, A. Farooq, K. Akhtar and A. M. Asiri, in *Handbook of Materials Characterization*, Springer International Publishing, 2018, pp. 317–344.
26 A. B. D. Nandiyanto, R. Oktiani and R. Ragadhita, *Indones. J. Sci. Technol.*, 2019, **4**, 97–118.
27 Q. Liu, Y. Pu, Z. Zhao, J. Wang and D. Wang, *Trans. Tianjin Univ.*, 2020, **26**, 273–282.
28 Y. Q. Wang, J. Su, F. Wu, P. Lu, L. F. Yuan, W. E. Yuan, J. Sheng and T. Jin, *Int. J. Nanomed.*, 2012, **7**, 693–704.
29 L. Bai, C. Li, X. Chen, H. Zhou, F. Zhang, H. Cheng, Y. Li and M. Zhou, in *E3S Web of Conferences*, EDP Sciences, 2023, vol. 416.
30 P. Mondal and J. L. Yarger, *ACS Omega*, 2022, **7**, 33423–33431.
31 Y. Ji, X. Yang, Z. Ji, L. Zhu, N. Ma, D. Chen, X. Jia, J. Tang and Y. Cao, *ACS Omega*, 2020, **5**, 8572–8578.
32 T. Bala, B. L. V. Prasad, M. Sastry, M. U. Kahaly and U. V. Waghmare, *J. Phys. Chem. A*, 2007, **111**, 6183–6190.
33 S. Cheng, D. Hou, C. Li, S. Liu, C. Zhang, Q. Kong, M. Ye, S. Wu and Y. Xian, *ChemistrySelect*, 2021, **6**, 4063–4066.
34 I. A. Mudunkotuwa, J. M. Pettibone and V. H. Grassian, *Environ. Sci. Technol.*, 2012, **46**, 7001–7010.
35 S. V. N. T. Kuchibhatla, A. S. Karakoti, D. R. Baer, S. Samudrala, M. H. Engelhard, J. E. Amonette, S. Thevuthasan and S. Seal, *J. Phys. Chem. C*, 2012, **116**, 14108–14114.
36 M. L. Avramescu, P. E. Rasmussen, M. Chénier and H. D. Gardner, *Environ. Sci. Pollut. Res.*, 2017, **24**, 1553–1564.
37 S. Dagadu Chavan and D. M. Desai, *World J. Adv. Res. Rev.*, 2022, **16**, 389–402.
38 G. Lavanya, M. Sunil, M. M. Eswarudu, M. Chinna Eswaraiah, K. Harisudha and B. Naga Spandana, *Int. J. Pharm. Sci. Res.*, 2013, **4**(4), 1280–1286.
39 N. S. Ramesh and R. Saraswat, *J. Emerg. Technol. Innov. Res.*, 2022, **9**(11), a417–a426.
40 W. Zhao, W. Zhang, Y. Liu, G. Q. Chen, R. Halim and H. Deng, *Sep. Purif. Technol.*, 2022, **300**, 121802.
41 I. Ortiz-Gómez, G. B. Ramírez-Rodríguez, L. F. Capitán-Vallvey, A. Salinas-Castillo and J. M. Delgado-López, *Colloids Surf., B*, 2020, **196**, 111337.
42 A. Mathaweesansurn, S. Thongrod, P. Khongkaew, C. M. Phechkrajang, P. Wilairat and N. Choengchan, *Talanta*, 2020, **210**, 120675.
43 A. M. Fekry, S. A. Abdel-Gawad, R. H. Tammam and M. A. Zayed, *Measurement*, 2020, **163**, 107958.
44 S. Kalasin, P. Sangnuang, P. Khownarumit, I. M. Tang and W. Surareungchai, *ACS Biomater. Sci. Eng.*, 2020, **6**, 5895–5910.
45 E. Saputra, *Sens. Int*, 2024, 100286.
46 S. Sadeghi and M. Hosseinpour-Zaryabi, *Microchem. J.*, 2020, **154**, 104601.
47 C. Xu, M. Zhang, S. Zhang, P. Wang, C. Lai, D. Meng, Z. Chen, X. Yi and X. Gao, *J. Chromatogr. B*, 2024, **1243**, 124210.
48 N. Ozbek and S. Akman, *Food Chem.*, 2016, **200**, 245–248.
49 J. M. S. Almeida, R. M. Dornellas, S. Yotsumoto-Neto, M. Ghisi, J. G. C. Furtado, E. P. Marques, R. Q. Aucélio and A. L. B. Marques, *Fuel*, 2014, **115**, 658–665.
50 J. Saurina, E. López-Aviles, A. Le Moal and S. Hernández-Cassou, *Anal. Chim. Acta*, 2002, **464**, 89–98.
51 X.-D. Li and Q.-Z. Zhai, *J Chem*, 2020, **2020**, 9232385.
52 L. F. Capitán-Vallvey, P. Alvarez de Cienfuegos-Gálvez, M. D. Fernández Ramos and R. Avidad-Castañeda, *Sens. Actuators, B*, 2000, **71**, 140–146.
53 M. Benamor and N. Aguerssif, *Spectrochim. Acta, Part A*, 2008, **69**, 676–681.
54 M. Tarara, P. D. Tzanavaras and G. Z. Tsogas, *Sensors*, 2023, **23**(1), 198.